Initial Assessment of TeF_6 Adsorption

Nuclear Technology Research and Development

Prepared for
US Department of Energy
Material Recovery and Waste Form Development Campaign

S. H. Bruffey, J. Richards, T. Davis

Oak Ridge National Laboratory

30 June 2021
ORNL/SPR-2021/2085

SUMMARY

Research and development that supports the management of off-gases from nuclear fuel reprocessing has historically been focused on the off-gas streams that arise from aqueous reprocessing technology. However, as Gen-IV reactor development pathways move toward deployment, alternative spent nuclear fuel (SNF) processing and disposition pathways have been considered more actively. This work is focused upon aspects of fluoride volatility (FV) processing. The versatility of this method for deployment against multiple types of spent fuel encourages the continued advancement of both the primary separations processes and the secondary processes, including waste treatment, material control and accountability, and engineering designs.

Recent work noted that TeF_6, the most highly volatile fluorinated compound produced during FV processing, did not have a clear abatement technology recommended in the literature. Thus, this work performed scoping tests on activated alumina and copper shot to assess whether they could be used to remove TeF_6 from gas streams that bear F_2. Previous work on this topic was not well described in the literature and was not performed with excess F_2 in the stream as would be typical of spent fuel processing via FV. To support an understanding of the concentration of TeF_6 contacting the adsorbent beds, a series of preliminary testing identified the TeF_6 production rate and the equilibrium concentration of TeF_6 in the gas stream contacting the adsorbent.

Excess F_2 was determined to not affect the ability of activated alumina to remove TeF_6 from the gas stream quickly and completely. A determination of whether excess F_2 affected the distribution depth of Te in the sorbent bed is still pending analysis of the used sorbent. Literature suggests that when activated alumina is near saturation, TeF_6 could migrate from the sorbent bed. Future testing should investigate this possibility.

Copper metal did not adsorb TeF_6 in the presence of F_2 across the sorbent temperature range of 50 to 335°C. F_2 was fully removed by the copper bed. Although preliminary thermodynamics would indicate adsorption to be energetically favorable, other factors that impact adsorption (e.g., slow kinetics, excess fluorine on the copper surface, an unfavorable transition state) are likely preventing the adsorption of TeF_6 at an easily measurable rate.

The work also investigated TeF_6 production from multiple forms of Te in the temperature range of 100 to 250°C. No previous study had assessed the initial reaction rates for this process. A carefully designed study allowed determination of the activation energy for the production of TeF_6 from Te metal.

The substantial amount of data collected during this study merits analysis beyond what is described here. A more in-depth kinetic analysis will be pursued. Additional analytical results will provide the ability to benchmark adsorption coefficients for TeF_6, understand the distribution of TeF_6 within the alumina bed, and better understand the effect of F_2 partial pressure on Te fluorination. The data from this report, as supplemented by these additional analyses, will be submitted to a peer-reviewed journal.

CONTENTS

FIGURES

TABLES

ACRONYMS

FTIR	Fourier-transform infrared spectroscopy
FV	fluoride volatility
ICP–MS	inductively coupled plasma–mass spectrometry
ORNL	Oak Ridge National Laboratory
SNF	spent nuclear fuel

INITIAL ASSESSMENT OF TeF_6 ADSORPTION

1. INTRODUCTION

Removing radionuclides from facility off-gas streams is important in the deployment of advanced nuclear technology. Limiting gaseous radiological emissions from reactors and fuel cycle facilities is critical for minimizing environmental contamination from a facility, ensuring that the dose received by the general public falls within regulatory limits and is as low as reasonably achievable and supporting the safe long-term disposition of radiological material associated with advanced fuel cycles.

Research and development that supports the management of off-gases from nuclear fuel reprocessing has historically focused on the off-gas streams that arise from aqueous reprocessing technology. However, as Gen-IV reactor development pathways move toward deployment, alternative spent nuclear fuel (SNF) processing and disposition pathways have been considered more actively. Although proposed processing technologies vary widely, several historical SNF processing concepts continue to merit consideration, and these technologies could be correlated to specific reactor designs. Most notably, the electrochemical processing of SNF is well-matched with the metallic fuel deployed in fast reactors, and the irradiated metal fuel is easily dissolved into the processing salt and the final metal product suited for fabrication as recycled metal fuel. Salt-fueled reactors, such as the molten chloride fast reactor or a fluoride salt-based thermal reactor, naturally lend themselves to volatility processing methods, recovering uranium from the fuel as either gaseous UCl_x or UF_6.

The subject of this work is fluoride volatility (FV) processing. FV methods were used successfully to defuel the spent fuel salt used in the Molten Salt Reactor Experiment at Oak Ridge National Laboratory (ORNL). Beyond that, FV has been a subject of international research and development for several decades as a processing technology used to recycle irradiated uranium oxide fuel (Collins, et al. 2018). The versatility of this method in deployment against multiple types of spent fuel encourages the continued advancement of both the primary separations processes and the secondary processes, including waste treatment, material control and accountability, and engineering designs. Figure 1 shows the concept of FV used for irradiated uranium oxide fuel assemblies, and Figure 2 shows the concept of FV used for irradiated uranium-bearing fuel salt.

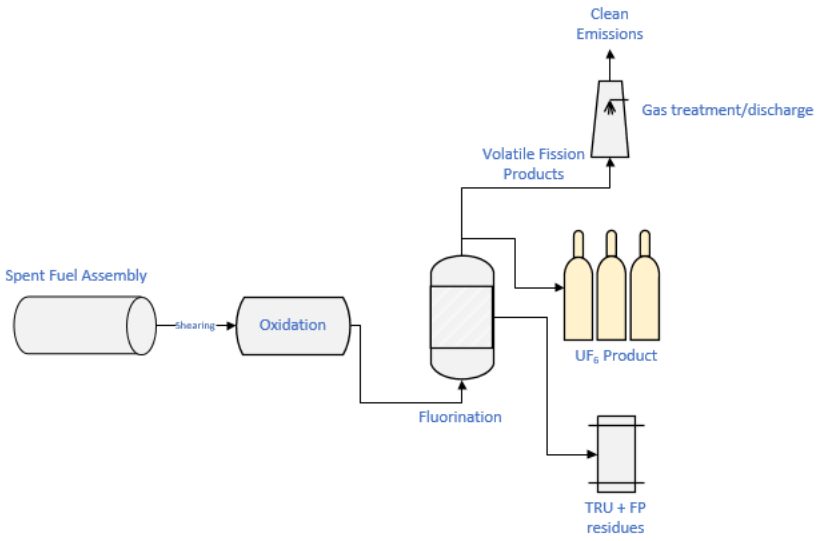

Figure 1. Processing uranium oxide fuel by FV.

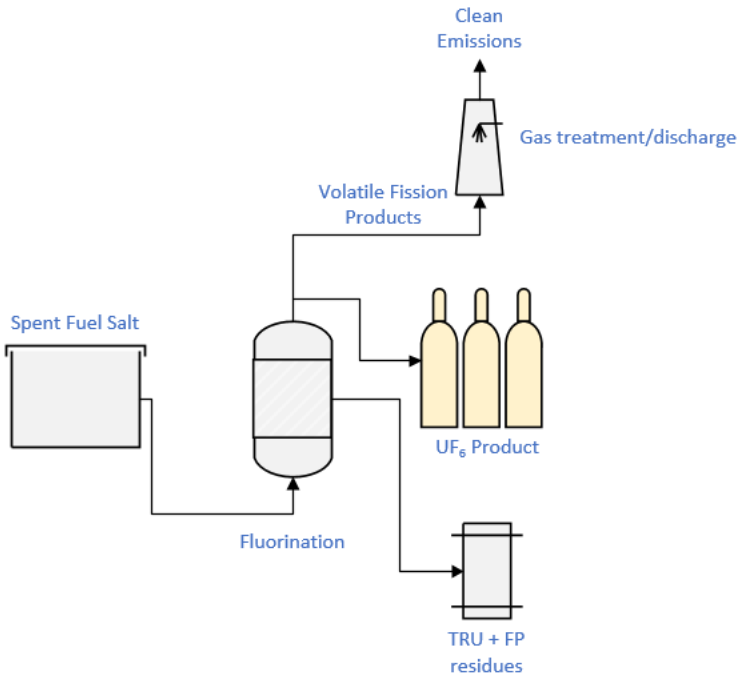

Figure 2. Processing uranium fuel salt by FV.

Volatility processing is especially interesting when considering the management of radioactive off-gas wastes as the product itself (UCl_x or UF_6) resides in the vapor phase with the contaminants of concern. Thus, off-gas treatment flowsheets will both purify the product and reduce radioactive emissions. Recently, a series of detailed mass balances were performed for the FV process represented in Figure 1 using an ORIGEN simulation of pressurized water reactor fuel (Catawba I type). The peak assembly

discharge burnup was 50 GWd/tU, and the average assembly discharge burnup was 40.2 GWd/tU. Three cycles of 395 days each were simulated with 20 day cycle downtimes. The selected cooling time was 15 years. The initial ^{235}U enrichment of the UO_2 fuel was set at 4.0%. The dataset was generated based on uranium fission only; no impurities were assumed to be present in the fuel. The results of this simulation and the associated mass balance identified the gaseous effluent from the fluorination step as being composed, as described in Table 1.

Table 1. Composition of process gas discharged from the fluorination of reference spent fuel.

Component	Mass of component present in off-gas stream (g/assembly)	Treatment step
CF_4	2.79E-03	n/r*
N_2	5.80E-05	n/r
Ne	7.87E-04	n/r
Br_2	9.08E+00	n/r[1]
Kr	6.44E+01	Storage as compressed gas
MoF_6	3.70E+03	n/r[2]
TcF_6	8.15E+02	MgF_2 sorbent
RuF_5	2.06E+03	Cryolite (Na_3AlF_6)
TeF_6	4.47E+02	To be determined
I_2	8.45E+01	Quench
Xe	9.69E+02	Storage as compressed gas
At_2	4.46E-20	n/r
Rn	4.76E-12	n/r
UF_6	5.81E+05	NaF recovery
F_2	Process gas	n/r[1]

* *n/r* stands for *abatement not required*
[1] Consumed during I_2 neutralization
[2] Consumes NaF during UF_6 recovery

As part of the mass balances development, separations technology for the radionuclides of concern were also reviewed. With the exception of UF_6, the capture technologies needed to support the management of gaseous components that arise from FV processing had very low technological maturity. Notably, the literature review did not identify any agreement as to the best capture methodology for TeF_6. This literature is discussed further in Section 2 of this report.

With an activity of 21.5 Ci/assembly at 15 years after reactor discharge, ^{125m}Te is formed from the decay of the fission product ^{125}Sb and is in transient and/or secular equilibrium with this parent, indicating that the activity will remain roughly constant until the Sb is sufficiently depleted (^{125}Sb $t_{1/2}$ = 2.76 years). The radiological half-life of ^{125m}Te is 57.4 days, and it undergoes internal transition, transforming to stable ^{125}Te.

Of the fluorinated compounds formed in FV, TeF_6 possesses the highest volatility, as shown in Table 2.

Table 2. Boiling points of key fluorinated compounds (Haynes, 2016).

Compound	Boiling point (°C)
TeF_6	−38.9 (sublimation point)
MoF_6	34.0
TcF_6	55.3
UF_6	56.5 (sublimation point)
RuF_5	227

2. BACKGROUND

To date, the earliest and most comprehensive evaluation of TeF_6 abatement was conducted by Vissers and Steindler (1968). In that work, the authors tested 13 sorbents: activated alumina, two types of charcoal, two types of molecular sieves, MgF, NaF, soda lime, CuO, and four metallic adsorbents, including Cu, Ni, Te, and Al. Gaseous radiolabeled TeF_6 was used as the TeF_6 source and the sorbent was contained in a 3.25 in. diameter tubular reactor with a maximum bed length of 12 in. All test system materials were nickel. Two types of experiments were conducted: (1) static batch-style sorption experiments and (2) flow-through sorption experiments.

In the batch-style experiments, the sorbent was placed into the heated sorption chamber, and a measured amount of TeF_6 was added into the evacuated chamber. The pressure of the system was monitored to track the pressure reduction, which was assumed to correspond to the sorption of TeF_6 by the sorbent. The excess TeF_6 was pumped off via a mild vacuum, and then the system was placed under a 10^{-2} Torr vacuum to remove any TeF_6 that was reversibly sorbed. These batch-style experiments were used to identify the most promising sorbents, which were then further investigated by flow-through sorption experiments. These sorbents included activated alumina, charcoal, and molecular sieve 13X. The flow-through sorption experiments indicated that alumina was the most desirable sorbent based on the decontamination factors achieved. Charcoal is no longer considered a desirable sorbent when F_2 is present because of the potential for uncontrolled reactions, and the flow-through experiments conducted in Vissers and Steindler using molecular sieve 13X did not validate the promise of the batch-style experiments.

Thus, a patent on the removal of TeF_6 via activated alumina was submitted (Vissers and Steindler 1970). This patent describes how excess F_2 can displace adsorbed TeF_6, indicating that the TeF_6 is adsorbed reversibly or that it could require a soaking period to fully immobilize on the adsorbent. Komaki et al. (1973) attempted to better understand TeF_6 sorption by activated alumina, but the experiments were conducted without excess F_2 and did not address the concern of TeF_6 removal or displacement from alumina.

Thus, the literature shows that activated alumina, the only sorbent studied in any detail, is still surrounded by unanswered questions regarding its TeF_6 sorption ability in realistic off-gas streams. Even if alumina is effective at absorbing TeF_6 in the presence of excess F_2 gas, much of the alumina's capacity would be used by co-adsorbed F_2, increasing the replacement frequency of absorbent cartridges and preventing the recycle of F_2 into the process, if recycle was desired.

The current work sought to evaluate TeF_6 sorption by activated alumina in the presence of excess F_2. Additionally, the concept of a TeF_6-selective sorbent was considered, and copper shot was tested for this purpose. Preliminary thermodynamic calculations indicate that progressive temperature ramping of the copper sorbent could promote selective TeF_6 removal by copper, but this had not been investigated until this work. To support an understanding of the concentration of TeF_6 contacting the sorbent beds, a series of

preliminary testing identified the TeF_6 production rate and the equilibrium concentration of TeF_6 in the gas stream that contacts the adsorbent.

3. METHODS

Three primary aims were completed through a series of eight tests. First, the rate of Reaction 1 was characterized to assess the dependence of the rate on temperature and particle size. The total amount of TeF_6 produced under process conditions was measured and used to determine the concentration of the TeF_6 streams used in sorbent testing.

$$\text{Reaction 1: } Te(s) + F_2(g) \rightarrow TeF_6(g)$$

Second, TeF_6 sorption by alumina was tested at two different F_2 concentrations to determine the effect of excess F_2 on TeF_6 sorption. Third, TeF_6 sorption by copper was determined as a function of temperature. The completed tests are shown in Table 3.

Table 3. Summary of completed tests.

Test	Reaction temperature (°C)	Sorbent (bed temperature, °C)	Particle size of Te (µm)	Comments
3	250	n/a	10–25	Unsieved Te metal F_2 addition in aliquots
4	200	n/a	10–25	F_2/N_2 not fully mixed before testing
5	100	n/a	10–25	
6	150	n/a	10–25	
7	150	n/a	37–74	
8	125	n/a	10–25	
9	200	Alumina (35)	10–25	Alumina not sufficiently activated
10	200	Alumina (35)	10–25	
11	200	Alumina (35)	10–25	40% F_2/N_2
12	200	Copper (50–335)	10–25	Used 60 mg Te

3.1 Test System

Handling F_2 gas necessitates specialized experimental equipment, an understanding of safe F_2 handling practices, and a fundamental understanding of corrosion, hydrolysis, and other common F_2 operational challenges. Additionally, TeF_6 is more toxic to humans than F_2 and has very low exposure limits. The equipment used supported the safe handling of all reagents. It is constructed primarily of stainless steel that has been passivated for use in F_2 handling. Stainless steel is not compatible with fluorine at high temperatures, so for higher temperature operations (>125°C), high nickel alloys (H-276 or Inconel-625) or Ni-coated reactors were required.

The test loop is represented in Figure 3. Primary components included a heated reactor used to produce TeF_6 from Te metal, a sorbent test column, a metal bellows recirculation pump, a vacuum pump, a flowmeter, pressure gauges, a mass flow meter, thermocouples within the reaction vessel, and a Fourier-transform infrared (FTIR) spectrometer. The total volume of the loop is assumed to be approximately 1 L. A picture of the entire test loop is shown in Figure 4, and the reaction vessel is shown in more detail in Figure 5. Figure 4 does not show the sorbent beds that were connected to the loop during tests 9–12. When

the inlet-side and effluent-side valves of the sorbent bed were open, the sorbent bed was in line with the test loop.

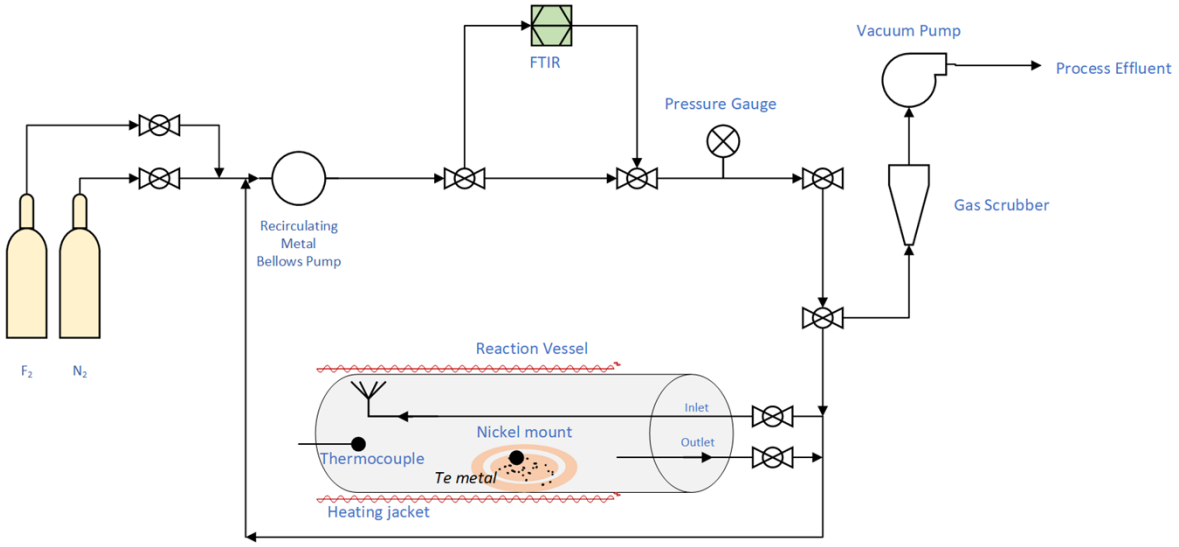

Figure 3. Test loop schematic.

Figure 4. Laboratory test loop.

Figure 5. Reaction vessel.

3.2 General Test Method

Each test followed a similar experimental method. First, approximately 30 mg of Te powder were transferred to a nickel plate and placed inside the reaction vessel and in the heating zone. If a sorbent bed was in use, then it was filled with adsorbent and placed in line with the test loop. The system was tested for large leaks and then evacuated and refilled with N_2 three times to remove any residual moisture. The system was then evacuated, and a formal leak check was performed. The system was assumed to be leak-tight if the leak rate was less than 0.01 Torr/min.

The reaction vessel and sorbent bed were brought to temperature, filled with 100 Torr N_2, and isolated from the recirculation loop. The recirculation loop was evacuated, filled with a 20% F_2 mixture made by combining 20 Torr F_2 with 80 Torr N_2. Tests 11 and 12 used a 40% F_2 mixture while maintaining the same overall pressure. The gas mixture was poorly mixed during early tests, so a 45–60 min recirculation period

was added after the gas was added to the test loop to ensure that the gas was well mixed before introducing it to the reaction vessel.

After gas mixing, the reaction vessel was opened to the recirculation loop. The reaction was monitored by FTIR with scans conducted as frequently as every 20 s. When FTIR measurements indicated that TeF_6 production was complete or plateaued, the gas flow was the circulated through the sorbent bed. FTIR monitored decreases in the TeF_6 concentration. When TeF_6 sorption was complete, the gas was discharged into a trapping bed, and the system was evacuated and refilled with N_2 three times before bringing to ambient pressure with N_2 and breaking the system. During testing, the reactor temperature and system pressures were continuously monitored.

The nickel plate located inside the reactor was retrieved, along with any unreacted Te metal. Images of the nickel plate and Te residue are shown in Figures 6 and 7. The orange coloring is attributed to possible silver fluoride compounds on the surface of the plate; Ag residue could be present on the plate post-manufacturing, and the plates were used as-received. Silver fluorides are hygroscopic, and some liquid was observed on the plate after removing it from the reactor, as shown in Figure 7. The residue was dissolved into 2% HNO_3. Drops of HF were added to each sample to promote the dissolution of any partially reacted Te, which could be in the form of TeF_x. This solution was analyzed by inductively coupled plasma–mass spectrometry (ICP–MS) to quantify the amount of Te unreacted in each test.

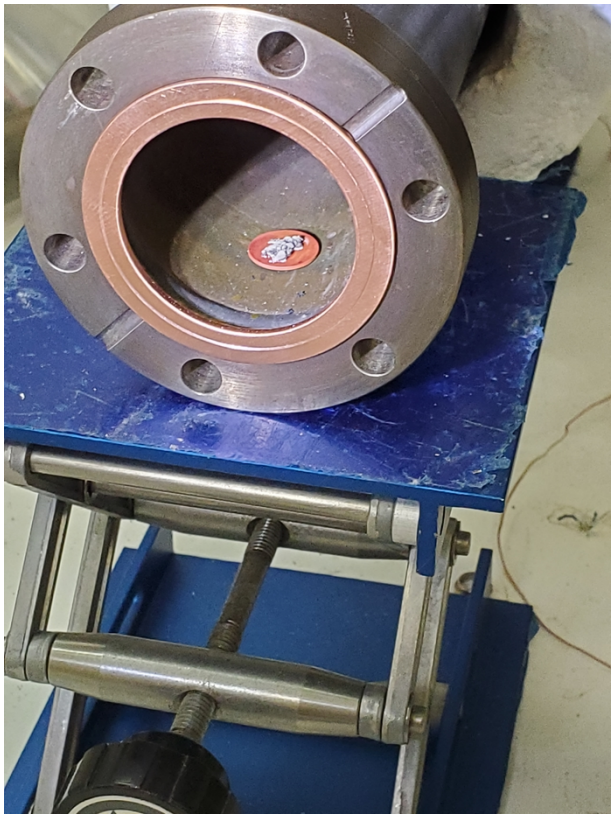

Figure 6. Te metal and Ni plate post-test.

Figure 7. Te residue post-test.

The sorbent beds were poured out in aliquots directly into glass vials. Each aliquot was weighed. The bed segments will be analyzed to determine the total Te adsorbed on each bed segment. This analysis is still pending.

3.3 FTIR Measurements

The infrared spectra were taken with an ABB MB3000 FTIR fitted with a 12 cm stainless-steel gas cell with ZnSe windows. All spectra were taken with a resolution of 4 cm^{-1} and were the average of five scans.

For each run, a background spectrum was collected while the system was under vacuum. A spectrum of the mixed F_2/N_2 was also collected before reaction initiation. After reaction initiation, TeF_6 is easily monitored by a strong peak at 752 cm^{-1}, as shown in Figure 8. There is a secondary TeF_6 band located at 889 cm^{-1}. The only other absorption bands of note are bands associated with trace HF (4,000 cm^{-1}) resulting from trace water within the test system and trace CO_2 (2,300–2,200 cm^{-1}).

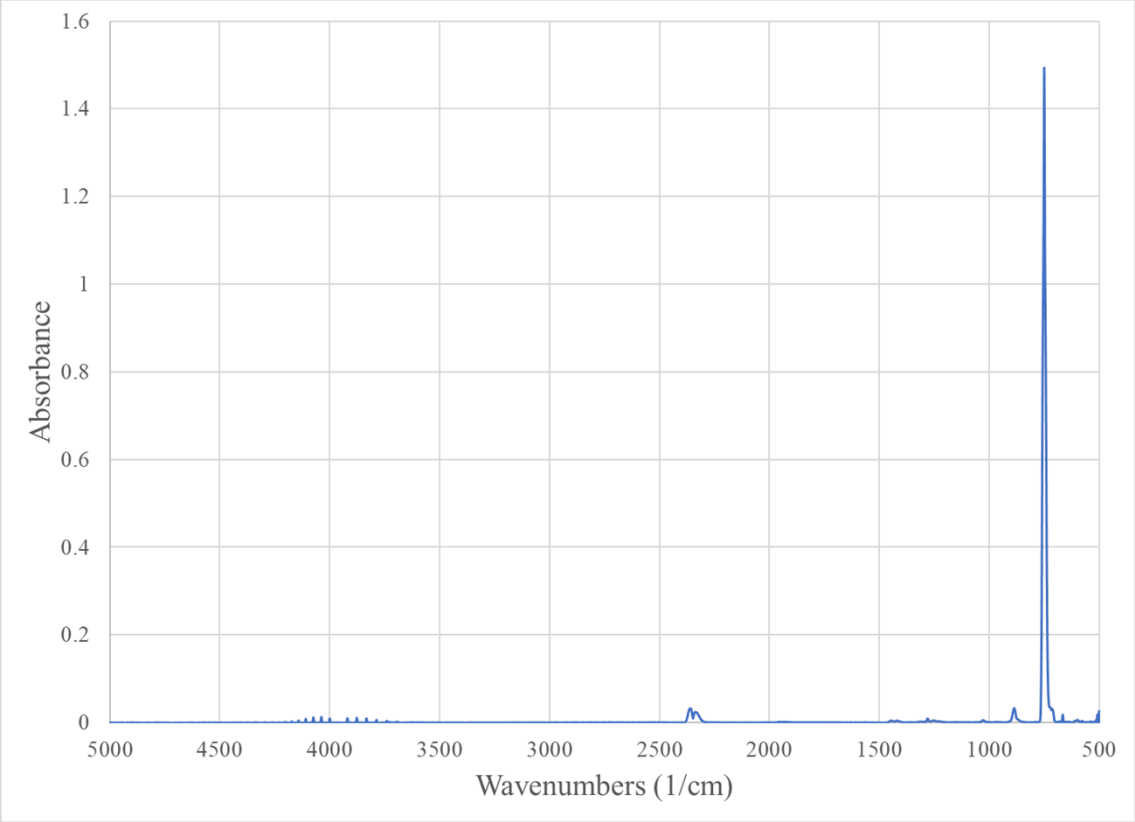

Figure 8. FTIR spectrum of TeF_6.

MacDowell et al. (1986) reported an absorptivity coefficient of 1,751 cm^{-2} atm^{-1}, or 2.3 cm^{-2} $Torr^{-1}$, for the TeF_6 peak of interest.

3.4 Materials

Te metal was from CERAC chemicals with a purity of >99.99%. It was sieved with commercially available sieves to separate particle size fractions of 10–25, 25–37, and 37–74 µm. F_2 gas was used as-received from Linde plc. Copper was purchased from Sigma-Aldrich as -20-+30 mesh shot with 99.95% purity.

The alumina was Delta F200 3/16 in. γ-alumina pellets. Prior to use, the alumina was dried at 100°C under flowing dry air before being crushed and ground in a mortar and pestle. Particle size was variable with no particles larger than 1 mm in diameter.

3.5 Sorbent Bed Design

Throughout the experiments described here, efforts were taken to minimize the amount of TeF_6 produced and thus reduce any potential exposure risk if system failures are encountered. For this reason, the sorbent beds themselves were sized relatively small. Each bed was 6 in. deep and held in passivated Inconel tubing with an inner diameter of ¼ in. Sorbent particle sizes were also small to minimize channeling and to maintain an appropriate sorbent particle diameter to bed diameter ratio. The sorbent tubes were heated with heat tape external to the tube. The sorbent material was supported by copper wool plugs at the effluent side of the column. The columns were held vertically with a downflow configuration.

4. RESULTS

Several preliminary tests not fully documented here resulted in the following findings. First, TeF_6 is not produced from TeO_2 under the test conditions used, although it is likely that at higher temperature ranges (beyond those tolerated by this test system) the reaction would occur. Second, the F_2/N_2 blend must be completely mixed before initiating TeF_6 production to accurately measure TeF_6 production rates. Third, the amount of F_2 provided to the reactor is sufficient to ensure the achievement of a relatively steady-state condition. Roughly, the amount of F_2 provided to the reaction was double the stoichiometric amount required for conversion of all Te to TeF_6.

FTIR data were used effectively to monitor the reaction rates and TeF_6 sorption in real time. The ingrowth of the TeF_6 peak is shown in Figure 9.

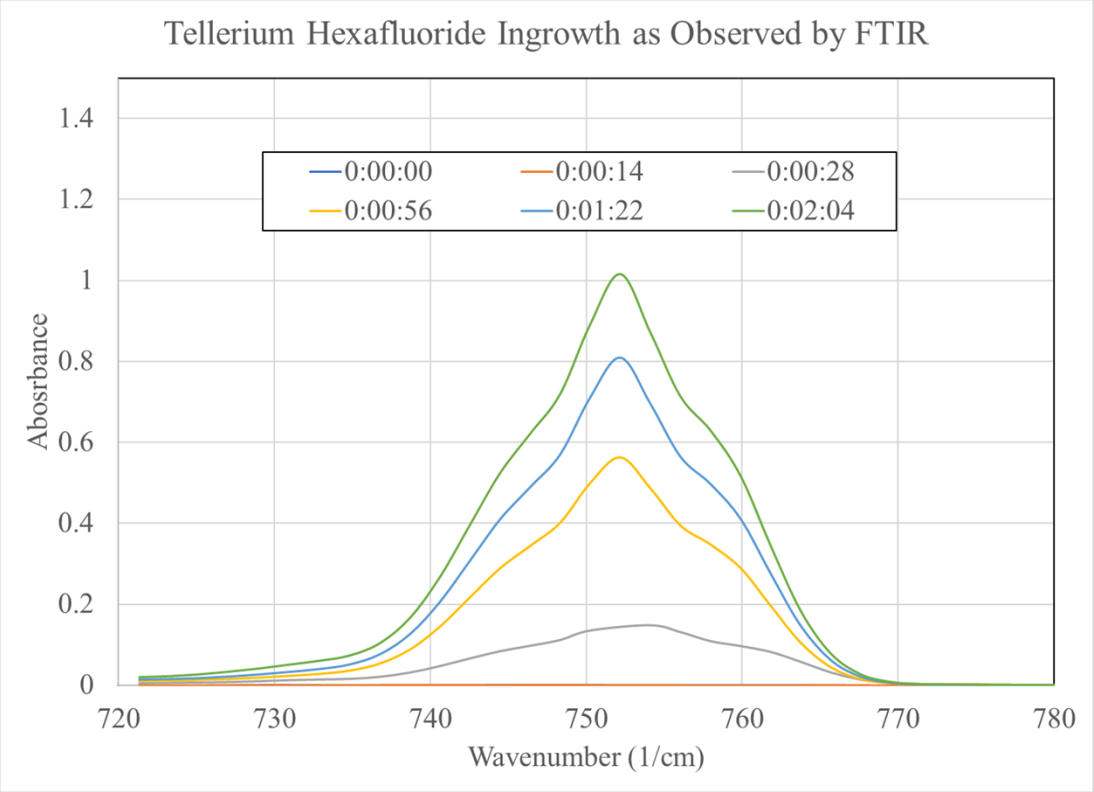

Figure 9. Ingrowth of TeF_6 as shown by successive FTIR scans. The legend indicates the time of each scan in minutes.

The maximum absorbance at 752 cm^{-1} was plotted as a function of reaction time, as shown in Figure 10, to determine the initial rate of reaction and whether the reaction was complete. Figure 10 also highlights the results of replicate testing at 200°C, showing that the initial rates of reaction are highly reproducible but that the total amount of TeF_6 produced varies, as reflected by the maximum absorbance. The total amount of Te reacted (and TeF_6 produced) may correlate with the available surface area of the metal, but additional data would be required to support this hypothesis.

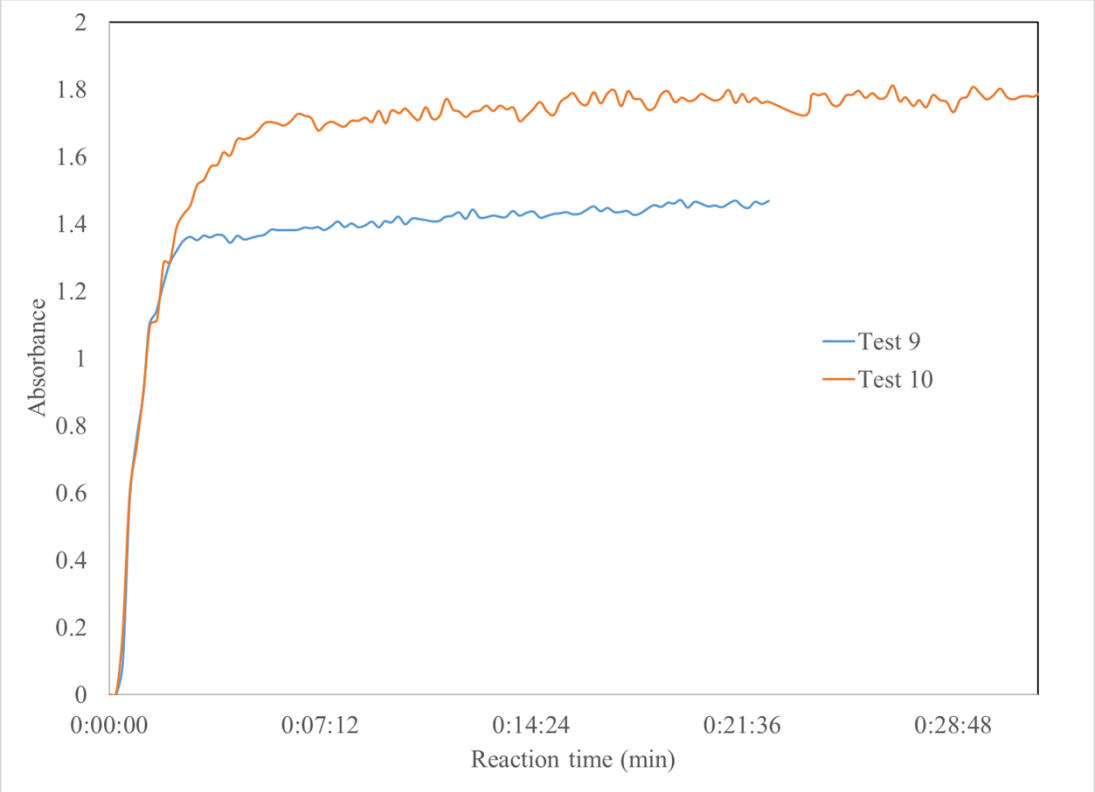

Figure 10. Monitoring of TeF_6 absorbance as a function of reaction time. TeF_6 produced at 200°C using 20% F_2 gas mixture.

4.1 TeF_6 Production Characteristics

Reaction 1 was examined to understand the effects of temperature (100–250°C), F_2 partial pressure (10–40 Torr), and Te particle size (10–25 and 35–74 µm) on the reaction rate and total TeF_6 produced.

4.1.1 TeF_6 Production Rate as a Function of Temperature

As shown in Figure 10, the production rate of TeF_6 plateaus less than 15 min after reaction initiation. The period ranging from 0 to 15 min is shown in Figure 11 for tests at the five examined temperatures. From this graph, it is evident that the test completed at 100°C did not produce TeF_6 at a rate similar to those of other temperatures.

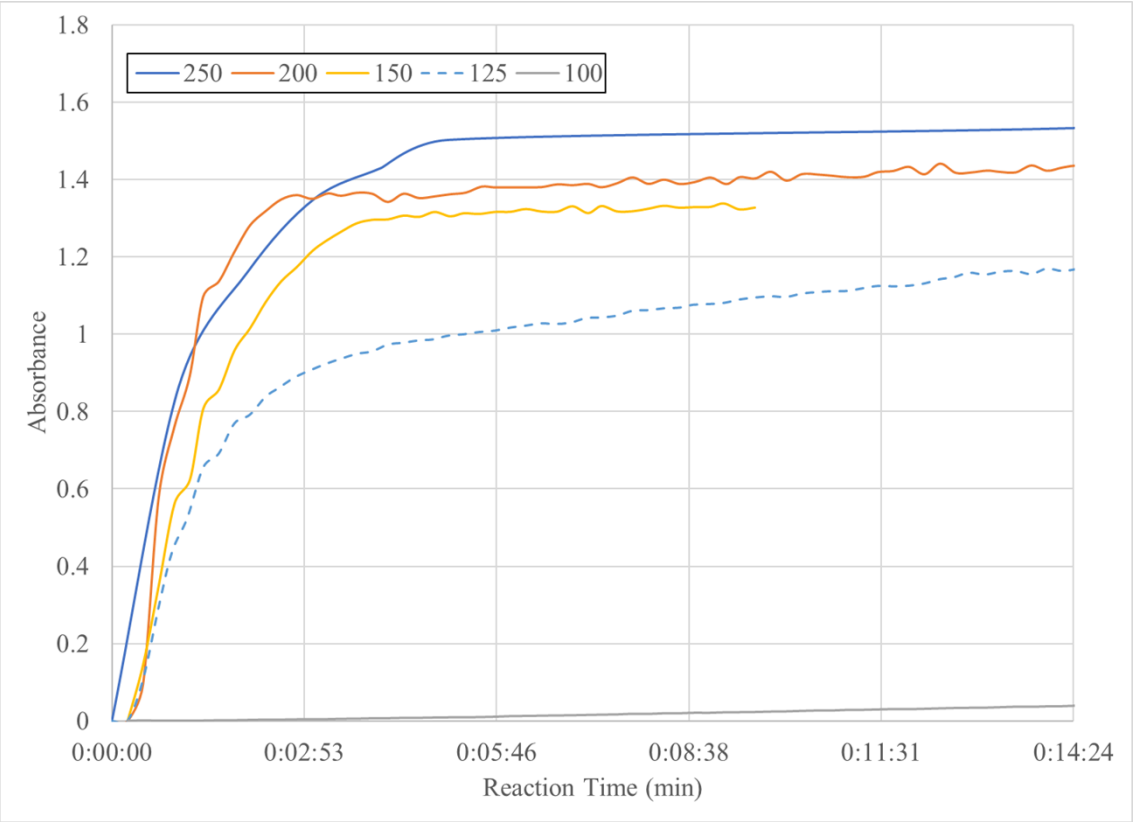

Figure 11. Initial TeF_6 production at varying temperatures for the period of 0–15 min.

The initial rate of reaction for the period of 0–2 min is shown in Figure 12. The data collected at 250°C are excluded because the F_2 concentration varied from that of runs 6, 8, and 9. The data shown in Figure 12 will be used for a subsequent formal kinetic analysis not documented here.

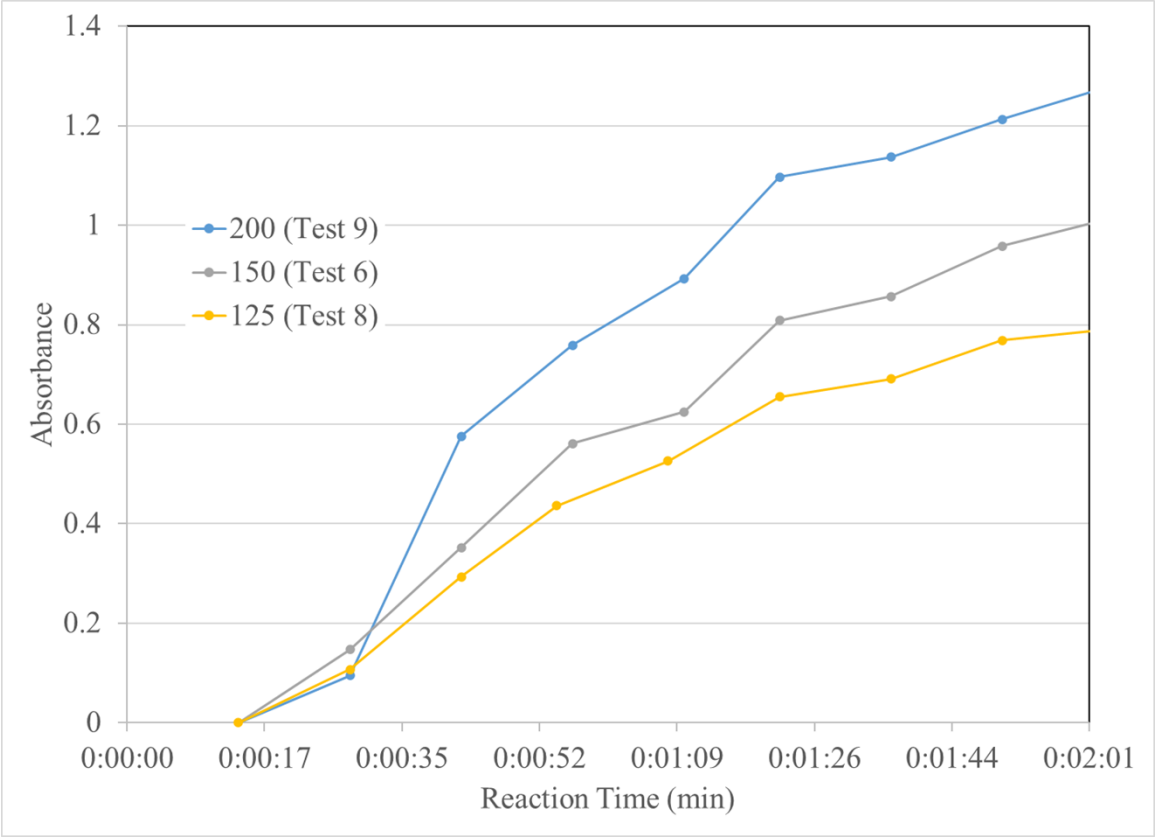

Figure 12. Initial reaction rate as a function of temperature.

The Arrhenius equation relates the reaction rate to the activation energy of the reaction by the equation:

$$k = Ae^{\frac{-E_a}{RT}}, \tag{1}$$

where k is the initial reaction rate, A is the constant pre-exponential factor, E_a is the activation energy, R is the ideal gas constant, and T is the temperature. The initial rate of reaction (k) can be determined using Eq. (2). This allow the activation energy to be determined for the Reaction 1 from the slope of a plot of ln(k) versus 1/T (Figure 13) as 9.83 ± 0.14 kJ/mol.

$$k_{00:14-02:04} = \frac{\Delta ABS_{t_{00:14-02:04}}}{\Delta t_{00:14-02:04}} \tag{2}$$

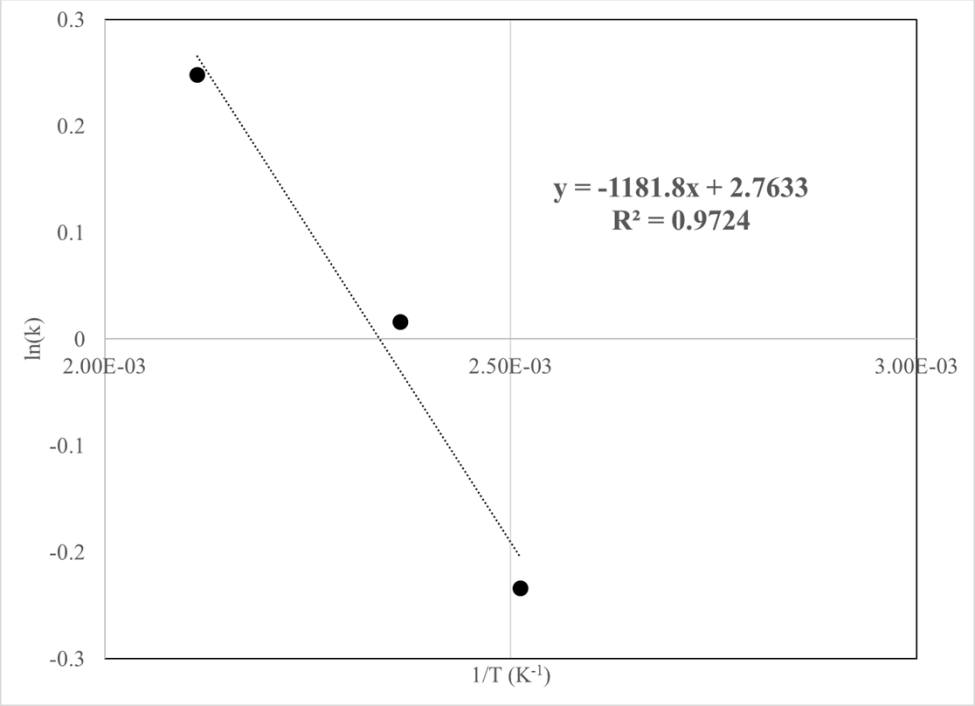

Figure 13. Arrhenius plot for reaction temperatures of 125–200°C.

4.1.2 TeF_6 Production Rate as a Function of Particle Size

While testing the two particle size ranges of interest (10–25 and 35–74 µm), these two size ranges were observed to behave differently during the transfer to the nickel plate used for support in the reaction vessel. The smaller size fraction clumped and aggregated together, whereas the larger size fraction poured easily, and individual particles could be individually distinguished visually. For these reasons, the Te metal arrangement on the nickel plate during the reaction was different for the two particle size fractions, mounds of Te metal were observed for the smaller particle size range, and the larger size range more evenly distributed in a flat layer on the plate.

TeF_6 production proceeded at 150°C, and the results are shown in Figure 14.

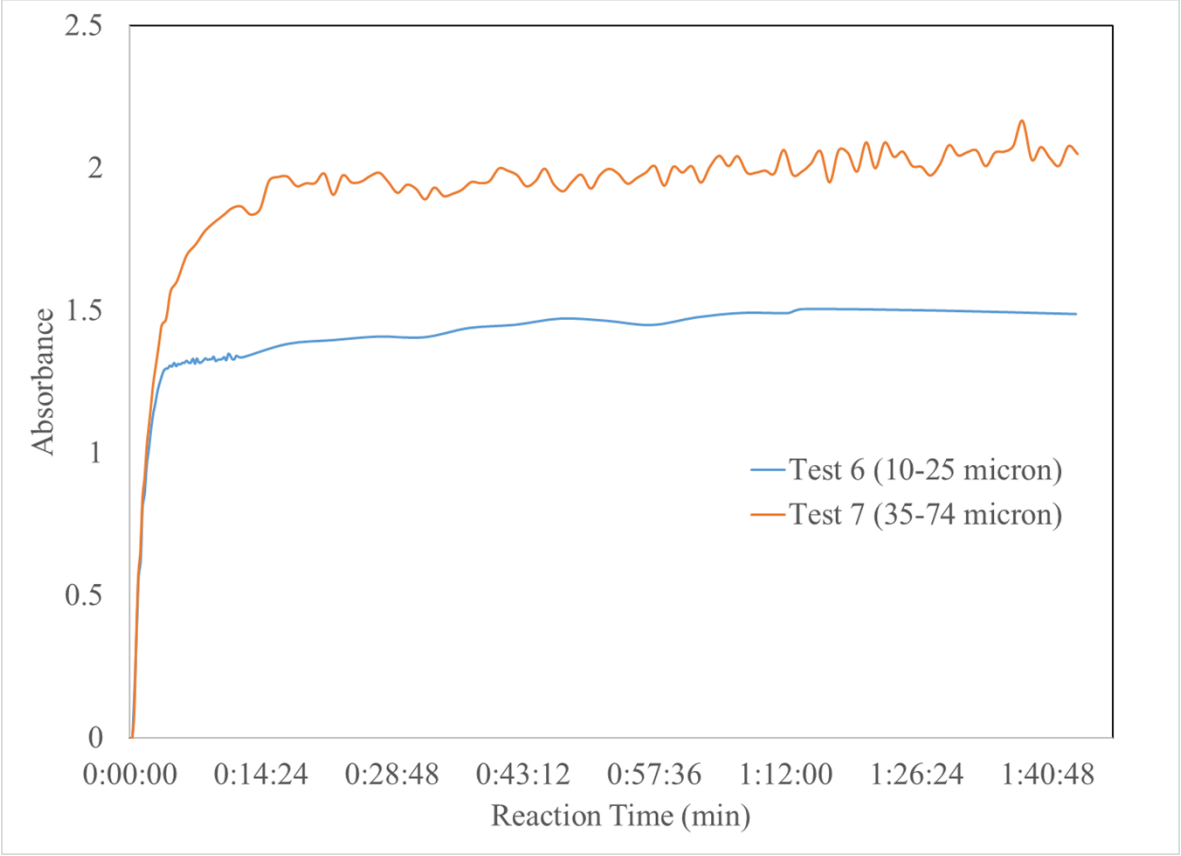

Figure 14. Production of TeF_6 from different particle size fractions.

Like in Figure 10, the initial reaction rates are nearly identical, despite the difference in particle size. However, the maximum absorbance is markedly different for the larger particle size, outside of the variability observed for production using 10–25 µm diameter particles. Although larger particle sizes typically reduce the area available for reaction, it is hypothesized in this case that the even distribution of the larger particle sizes on the nickel plate might have resulted in a larger accessible surface area for reaction.

4.1.3 TeF_6 Production Rate as a Function of Fluorine Partial Pressure

A scoping test was performed to evaluate whether increased F_2 partial pressure would result in an increased initial reaction rate. The results shown in Figure 15 indicate that the initial rate of reaction increases with an increase of F_2 partial pressure from 20 to 40 Torr. As observed in Figure 10, the total amount of Te volatilized per run (as reflected by the maximum absorbance) varied but the initial rates of reaction for replicate runs were constant.

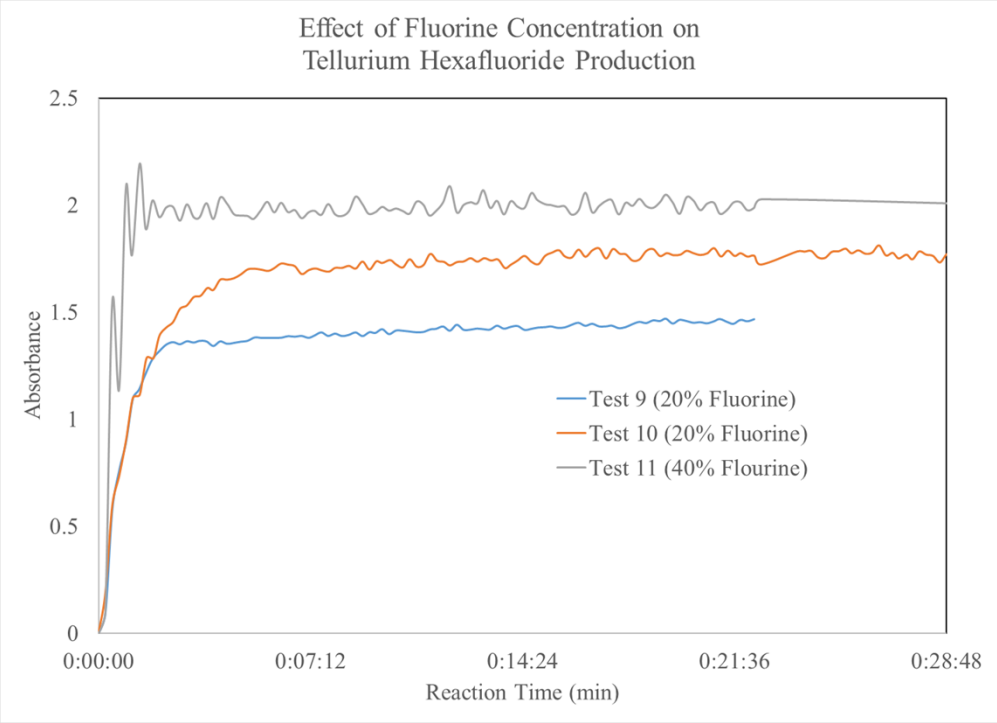

Figure 15. Effect of increased F_2 partial pressure on the initial reaction rate.

4.1.4 Mass Balances

The unreacted solids were recovered from each test, and the mass of Te in these solids was determined by the dissolution of the solids and analysis of the solution by ICP-MS for tests 3–10. These results are still under analysis. The amount of recovered solids was about 5 mg for each test that used 10–25 µm diameter Te metal particles. Less material was recovered from test 7 (using 25–37 µm diameter material) and from tests 9-10 (using higher F_2 concentrations). The amount of Te volatilized was inferred from the amount of Te recovered from the reaction vessel at the conclusion of each test and is shown in Table 4.

Table 4. Fraction of Te volatilized based on the mass of recovered solids.

Test	Initial Te mass (mg)	Recovered solids (mg)	Te volatilized (%)
3	29.4	5.67	80.7
4	29.3	5.28	82.0
5	28.0	Not recovered	–
6		5.97	
7	30.0	0.81	97.3
8		5.18	
9	29.0	3.05	89.5
10	32.6	3.32	89.8

4.2 TeF_6 Sorption

Tests 9–12 examined the sorption of TeF_6 by alumina and Cu. Test 9 used nonactivated alumina, which greatly decreased capacities for both F_2 and TeF_6, and those results are not reported here.

4.2.1 Sorption by Activated Alumina

FTIR data from test 10, shown in Figure 16, reflect a sharp production curve to a steady-state absorbance of about 2.0 and a subsequent sharp drop in absorbance to 0 as an activated alumina bed is placed in line with the test loop and TeF_6 is absorbed. Sorption of TeF_6 occurs very quickly and is complete. Sorption of F2 occurs concurrently and all F_2 is removed, as indicated by pressure monitoring on the system.

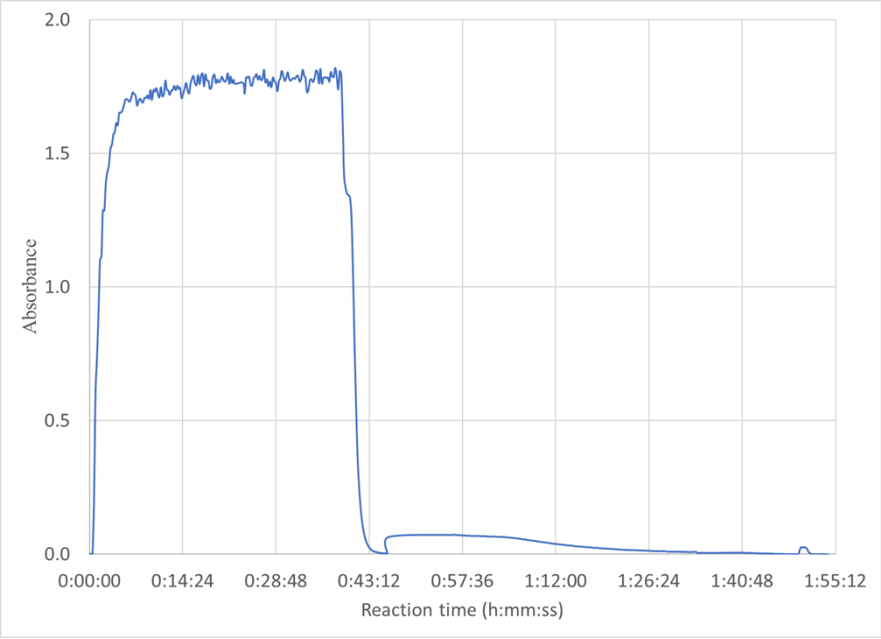

Figure 16. Production, steady-state, and sorption phases of test 10.

To assess how F could impact the sorption of TeF_6 by alumina, test 11 contained double the amount of F_2 as test 10 (40 vs. 20 Torr, respectively). The sorption phases of the two tests are compared in Figure 17. Although the two sorption curves are not identical, they both show near-complete sorption of TeF_6 within 6 min, and no deleterious effect on TeF_6 sorption was observed in the presence of higher F_2 pressures. Pending data on Te distribution through the alumina beds will provide information on whether the additional F_2 might affect TeF_6 penetration into the sorbent bed. In the tests completed here, the number of alumina sites available for reaction dwarfed the amount of TeF_6 and F_2 present. Future work should consider operating at conditions closer to sorbent saturation.

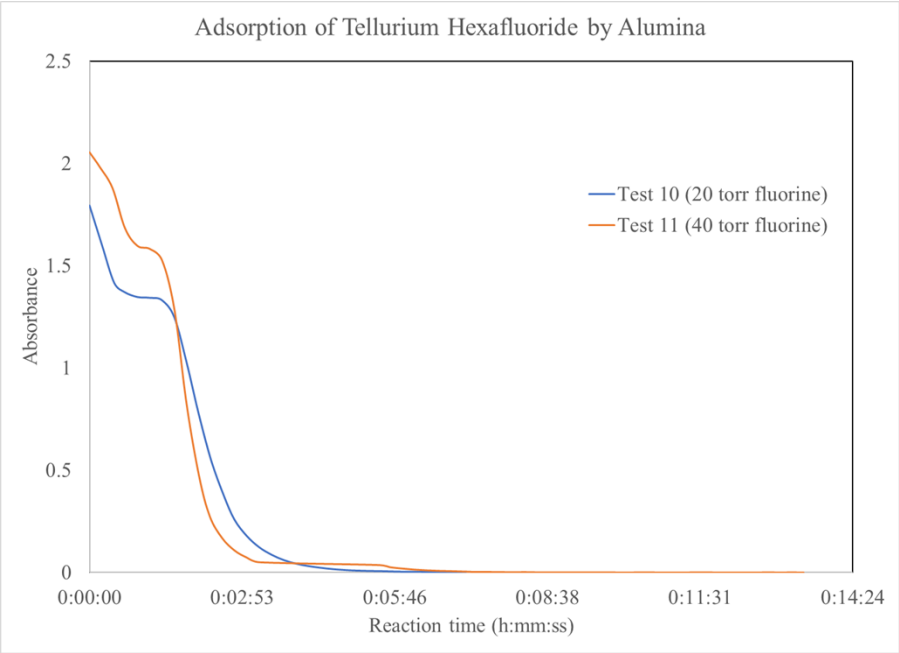

Figure 17. Sorption of TeF_6 by activated alumina at two different F_2 pressures.

4.2.2 Sorption by Copper

Vissers and Steindler (1968) indicated that Cu would absorb TeF_6, but details on sorbent temperatures and other specifics were not provided. Preliminary calculations were performed using HSC Chemistry to assess whether TeF_6 sorption was thermodynamically favorable and whether TeF_6 could be sorbed at different temperatures than F (Outotec 2018). Table 5 shows some potential sorption reactions and their free energies (ΔG_{rxn}). Because the potential sorption mechanism and resulting products were unknown, several different reactions were calculated with products, including CuTe, TeF_4, and CuF_2. These calculations showed that the decomposition of TeF_6 by Cu was thermodynamically favorable for some reaction pathways.

Table 5. Free energies of reaction for selected TeF_6 and F_2 interactions with Cu.

Reaction	ΔG at 100°C (kcal)
$F_2(g) + Cu \rightarrow 2CuF$	-121.6
$F_2(g) + Cu \rightarrow CuF_2$	-115.6
$TeF_6(g) + Cu \rightarrow CuTe + 3F_2(g)$	291.7
$TeF_6(g) + Cu \leftrightarrow TeF_4(g) + CuF_2$	-32.1
$TeF_6(g) + 3Cu \rightarrow 3CuF_2 + Te$	-48.4

Similarly, HSC Chemistry was used to generate predominance diagrams by using the three elements of interest: Cu, Te, and F. These predominance diagrams show a clear increase in the predominance of CuTe with temperature, as shown in Figures 18 and 19.

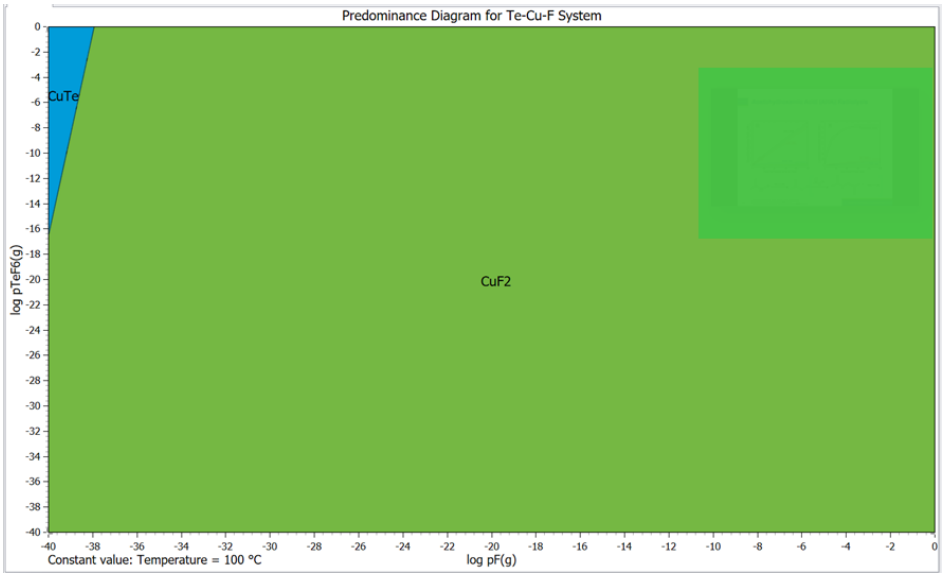

Figure 18. Predominance diagram for the Cu-Te-F system at 100°C.

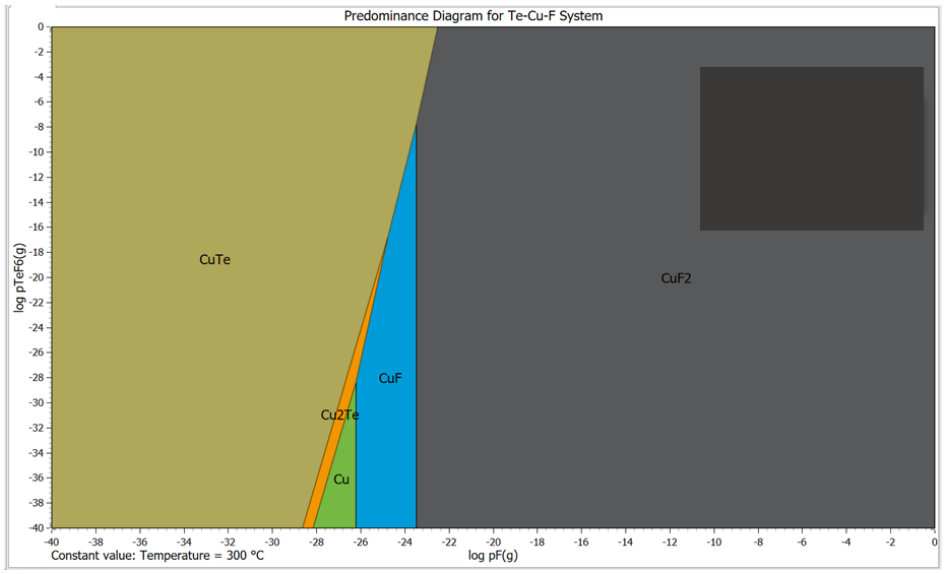

Figure 19. Predominance diagram for the Cu-Te-F system at 300°C.

Thermodynamic calculations cannot resolve the effects of two competing adsorbates because the reactions will be governed by not only the free energy of the reaction but also the kinetics of the reaction for the competing species' sorption and decomposition—in this case, TeF_6 and F_2. However, these calculations were favorable and suggested completing a scoping test to assess the behavior of TeF_6 in contact with a copper sorbent at varying temperatures.

This scoping test generated TeF_6 at 200°C and allowed the TeF_6 concentration to plateau. Once this occurred, the recirculating TeF_6/F_2 stream was passed through a copper sorbent bed while the total pressure of the system and the TeF_6 absorbance were monitored. The copper sorbent bed was ramped in stepwise fashion with hold times of about 10 min per step (50–335°C). The temperature profiles of the reactor and the copper sorbent tube are shown in Figure 20, and each temperature increment is designated with the letters A–K.

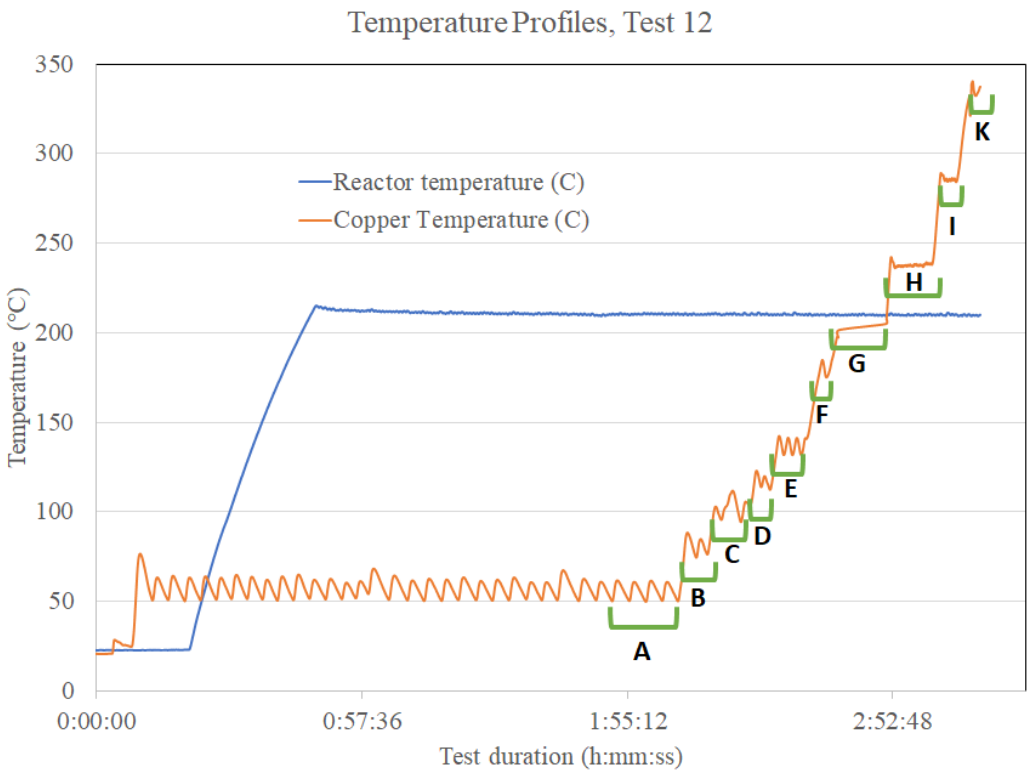

Figure 20. Temperature profiles of test 12 with each sorbent temperature hold noted as the letters A–K.

The system pressure dropped continuously during sorption testing, but the TeF_6 absorbance remained constant across all temperature steps. This indicates the sorption of F_2 with no sorption of TeF_6. For simplicity, only the FTIR scans for sorption phases A and K are shown in Figure 21, which reflect the constant TeF_6 absorbances across the test duration. The absorbances shown in Figure 21 are from the secondary TeF_6 peak (889 cm^{-1}) because the absorbance was greater than 3 for the primary peak due to the high amount of Te used in the experiment (60 mg vs. 30 mg for all other runs).

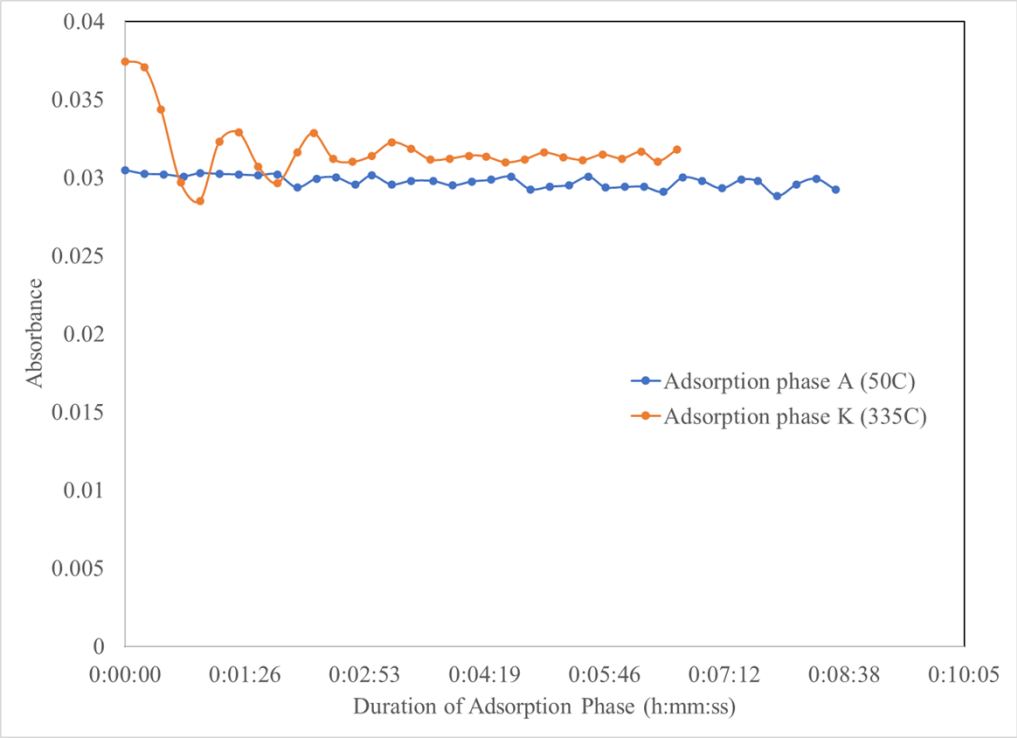

Figure 21. Comparison of TeF_6 absorbances during sorption phases A and K.

5. CONCLUSIONS

This work resulted in better understanding the potential of two common materials—activated alumina and copper to remove TeF_6 from gas streams that bear F_2. Previous work on this topic was not well described in the literature and was not performed with excess F_2 in the stream as would be typical of FV spent fuel processing.

Excess F_2 was determined to not affect the ability of activated alumina to remove TeF_6 from the gas stream quickly and completely. The determination of whether excess F_2 affected the distribution of Te in the sorbent bed is still analysis of the used sorbent. Literature suggests that when activated alumina is near saturation, TeF_6 could migrate from the sorbent bed. Future testing should investigate this possibility.

Copper metal was not found to adsorb TeF_6 in the presence of F_2 across the sorbent temperature range of 50 to 335°C. Although preliminary thermodynamics indicate that sorption is energetically favorable, other factors that affect sorption (e.g., slow kinetics, excess F_2 on the copper surface, an unfavorable transition state) are likely preventing the sorption of TeF_6 at an easily measurable rate.

Included in this effort was an analysis of TeF_6 production from Te metal in the temperature range of 100 to 250°C. No previous study had assessed the initial reaction rates for this process. A carefully designed study allowed activation energy for the production of TeF_6 to be determined from Te metal, and the particle size of the starting Te was determined to not affect the initial reaction rate.

The substantial amount of data collected during this study merits analysis beyond what is described here. A more in-depth kinetic analysis will be pursued. Additional analytical results will provide the ability to benchmark sorption coefficients for TeF_6, understand the distribution of TeF_6 within the alumina bed, and

better understand the effect of F_2 partial pressure on Te fluorination. The data from this report, as supplemented by these additional analyses, will be submitted to a peer-reviewed journal.

6. REFERENCES

Collins, E. D., et al. *State-of-the-Art Report on the Progress of Nuclear Fuel Cycle Chemistry* (No. NEA--7267). Organisation for Economic Co-Operation and Development. 2018

Haynes, W. M. (2016). *CRC Handbook of chemistry and physics: A ready reference book*. CRC Press: Boca Raton, FL, USA.

Komaki, Y., M. Iwasaki, and S. Tsujimura. "Removal of Volatile Tellurium Fluoride in Low Concentrations by Activated Alumina." *Journal of Nuclear Science and Technology* 10, no. 6 (1973): 385–387.

McDowell, R. S., R. F. Holland, W. H. McCulla, G. K. Anderson, and M. J. Reisfeld. "Infrared Spectroscopy of TeF_6." *Journal of Molecular Structure* 145, no. 3-4 (1986): 243–256.

Outotec, H. S. C. "Chemistry Software." Version 9, 1974–2018.

Vissers, D. R., and M. J. Steindler. "Removal of Tellurium Hexafluoride from Gaseous Systems by Solid Reagents." *Industrial & Engineering Chemistry Process Design and Development* 7, no. 4 (1968): 496–502.

Vissers, D. R., M. J. Steindler, and J. T. Holmes. 1970. Tellurium hexafluoride removal method. US Patent 3,491,513, filed October, 22, 1970, and issued January 27, 1970.